Hindawi Publishing Corporation
Journal of Nanomaterials
Volume 2015, Article ID 540247, 8 pages
http://dx.doi.org/10.1155/2015/540247

Research Article

The Comparative PDT Experiment of the Inactivation of HL60 on Modified TiO_2 Nanoparticles

Kaiqi Lu,[1] Qiyun He,[1] Li Chen,[2] Baoquan Ai,[1] and Jianwen Xiong[1]

[1]*Laboratory of Quantum Information Technology, School of Physics and Telecommunication Engineering, South China Normal University, Guangzhou 510006, China*
[2]*School of Physics and Optoelectronic Engineering, Guangdong University of Technology, Guangzhou 510006, China*

Correspondence should be addressed to Jianwen Xiong; jwxiong@scnu.edu.cn

Received 24 February 2015; Revised 24 May 2015; Accepted 10 June 2015

Academic Editor: Paulo Cesar Morais

Four samples of modified titanium dioxide (TiO_2), Fe/TiO_2 (2 wt%), Fe/TiO_2 (5 wt%), and 5-ALA/TiO_2, were experimented in photodynamic therapy (PDT) on leukemia cells HL60, performing promising photocatalytic inactivation effect. Fe/TiO_2 and 5-ALA/TiO_2 were synthesized in methods of precipitation and ultrasonic methods, respectively. X-ray diffraction spectra and UV-Vis spectra were studied for the samples' crystalline phase and redshift of absorption peak. Further, FTIR spectra and Raman spectra were obtained to examine the combination of 5-aminolevulinic (5-ALA) and TiO_2 nanoparticles. The toxicity of these four kinds of nanoparticles was studied through darkroom experiments. And based on the concentration which caused the same toxic effect (90%) on HL60, PDT experiments of TiO_2, Fe/TiO_2 (2%), Fe/TiO_2 (5%), and ALA/TiO_2 were done, resulting in the fact that the photokilling efficiency was 69.7%, 71.6%, 72%, and 80.6%, respectively. Scanning electron microscope (SEM) images of the samples were also taken to study the morphology of HL60 cells before and after PDT, resulting in the fact the activation of the modified TiO_2 from PDT was the main cause of cell apoptosis.

1. Introduction

Titanium dioxide (TiO_2) has been widely used in biomedical, industrial, environmental, and energy technology fields during the past two decades on account of its chemical and physical property [1]. For instance, iron and chromium doped TiO_2 nanotube had a promising effect on the degradation of environmental and industrial pollutants [2]. Ag/TiO_2 nanoparticles showed great photocatalytic effect on the degradation of water pollutions [3]. Wang and his team pointed out that TiO_2 based photocatalytic process for purification of polluted water had bridged fundamentals to applications [4]. It has been proven that pairs of photo-induced electrons and holes generated on the surface of TiO_2 under the irradiation of ultraviolet (UV) light [5, 6] performed strong reduction and oxidation power and could react with hydroxyl ions and water to form various reactive oxygen species (ROS) which played an important role in photodynamic therapy (PDT) [7–9].

In spite of its tremendous effect on killing cancer cells, the application of TiO_2 in PDT was hindered by a few of its properties. TiO_2, with the band gap of 3.23 eV for anatase, turned excited only when exposed to UV light; furthermore, the activated electron-hole pairs had a high speed rate of recombination, which would weaken the promising photocatalytic effect in PDT [10, 11]. Seeing its potential practical use, a wealth of researches had been done on the method of modification to enhance the efficiency of TiO_2 treatments on cancer cells and received sound results. Pt-TiO_2 has been demonstrated effective in treatment of localized tumors [12]. ZnPc-TiO_2 has been proved an excellent candidate as sensitizer in PDT against cancer and infectious diseases [13]. Water-dispersed TiO_2-polyethylene glycol compound had high antitumor effect in PDT [14]. Other modified TiO_2 nanoparticles such as N-TiO_2, Er^{3+}-Yb^{3+}-Fe^{3+} tridoped TiO_2, and Au/TiO_2 had been proved to have higher photocatalytic effect than pure TiO_2 on tumor cell [15–18]. Our laboratory had made some progress on tests of *in vitro* PDT based on modified TiO_2 such as CdS doped TiO_2, Fe-N codoped TiO_2, and TiO_2-xNx [19, 20].

In this paper, four kinds of nanoparticles (including TiO_2, Fe/TiO_2 (2 wt%), Fe/TiO_2 (5 wt%), and 5-ALA/TiO_2) were applied in PDT experiments on leukemic HL60 cells. Each dose was used and tested separately for PDT and toxicity experiments, and the comparison of cell viability between each independent experiment has been specifically studied, and this possible use of the experimental nanoparticles will be discussed at the end of this paper.

2. Materials and Methods

2.1. Chemicals and Apparatus. HL60 cells were kindly provided by the Department of Medicine of Sun Yat-sen University. 5-aminolevulinic acid (ALA) was purchased from Shanghai Xianhui Pharmaceutical Co. Ltd. (CHN). TiO_2 nanoparticles were purchased from Degussa (GER). RPMI medium 1640 was obtained from Gibco BRL (USA). Cell Counting Kit-8 (CCK-8) assays were purchased from Dojindo (Japan). Fe/TiO_2 (2%) and Fe/TiO_2 (5%) nanoparticles were synthesized in the method of precipitation by Department of Physics and Electronic Engineering of South China Normal University. 5-ALA/TiO_2 nanoparticles were synthesized by author's laboratory. All chemicals were of the highest purity commercially available. The tock solutions were well prepared in serum-free medium before use and materials stored in sealing space at a proper temperature.

The apparatus used included UV-2550 UV-visible spectrophotometer (Hitachi, Japan), HH.CP-TW80 CO_2 Incubator, DG5031 ELISA Reader (Nanjing Huadong Electronics Group Medical Equipment Co., Ltd., China), BS124S Electronic Scales (Sartorius, GER), SK2510LHC Ultrasonic Cleaner (KUDOS, China), SW-CJ Standard Clean Bench (Suzhou Antai Airtech Co., Ltd., China), LPE-1A Laser Power Meter (Physcience Opto-Electronics, Beijing), Eppendof (Finland), lab-assembled PDT light reaction chamber, 96-well culture plates, cell counting boards, and so on.

2.2. Cell Culture. Leukemia HL60 cells were cultured in RPMI 1640 medium with 10% fetal bovine serum (FBS) and refreshed daily. They were stored in a humidified incubator with 5% CO_2 at 37°C before use. In order to maximum the reliability of PDT effect, cells viability will be measured using a countess automated cell counter, verifying their sound concentration over 95%.

2.3. Preparation of Modified TiO_2 Nanoparticles

2.3.1. Synthesis of 5-ALA/TiO_2. 5-ALA/TiO_2 nanoparticles were synthesized in a way of surface modification. 2.62 mg 5-ALA and 3.2 mg TiO_2 nanoparticles were measured by an electronic scale and then dissolved in 20 mL deionized water contained with a beaker. Subsequently, the beaker was then sealed, vibrated using a magnetic stirrer, and placed in ultrasonic heater for an ultrasonic processing of 4 h. In this process, carboxyl groups on 5-ALA were believed to bond with the hydrogen bonds on TiO_2 nanoparticles. In this way, the 5-ALA/TiO_2 nanoparticles with a molar mass ratio (5-ALA : TiO_2) of 2 : 1 were synthesized.

2.3.2. Synthesis of Fe/TiO_2. $Ti(SO_4)_2$, $C_{18}H_{29}NaO_3S$ (DBS), H_2NCONH_2, deionized water, CH_3CH_2OH, and concentrated H_2SO_4 were compounded together in doses of 6 g, 0.18 g, 32 g, 250 mL, 0.25 mL, and 0.25 mL, respectively, with a certain dose of $Fe_2(SO_4)_3$; 0.1 g $Fe_2(SO_4)_3$ was applied to obtain Fe/TiO_2 (2%) and 0.5 g to Fe/TiO_2 (5%). The beaker of the reactant was put in 80°C thermostatic bath, quickly stirred for 2 to 3 hours until the PH value of the reactant reached 2. Then another 24 hours were taken for its complete sedimentation. Subsequently, SO_4^{2-} and the activator on the surface of DBS were washed away using deionized water until there was no $BaSO_4$ produced when $BaCl_2$ solution was tentatively added. CH_3CH_2OH was added to dehydrate the sample. After 3-hour desiccation in drying oven, our sample was grinded for 15 minutes in an automatic desktop grinder and then sintered for 30 minutes in a high temperature electric furnace at 450°C. When the sample cooled down, it was grinded again for 15 minutes and collected for use. The involved chemical equations were listed below:

$$
\begin{aligned}
Ti(SO_4)_2 + H_2O &\longrightarrow TiOSO_4 + H_2TiSO_3 \downarrow \\
CO(NH_2)_2 + 3H_2O &\longrightarrow 2NH_4^+ + 2OH^- + CO_2 \uparrow \\
Ti^{4+} + 2OH^- &\longrightarrow Ti(OH)_4 \downarrow \\
TiO^{2+} + 2OH^- &\longrightarrow TiO(OH)_2 \downarrow \\
① H_2TiSO_3 &\longrightarrow TiO_2 + H_2O \\
② Ti(OH)_4 &\longrightarrow TiO_2 + 2H_2O \\
③ TiO(OH)_2 &\longrightarrow TiO_2 + H_2O \\
Fe^{3+} + OH^- &\longrightarrow Fe(OH)_3 \downarrow \\
2Fe(OH)_3 &\longrightarrow Fe_2O_3 + 3H_2O
\end{aligned}
\tag{1}
$$

2.4. CCK-8 Assay. Cell viability of the samples was evaluated by Cell Counting Kit-8 assays (CCK-8 assay) [21]. Cell suspension was seeded into 96-well plate. Each well contained 200 μL HL60 cell suspension and 20 μL CCK-8 solution. The 96-well plates then were placed in an incubator (37°C 5% CO_2) for 4 hours before the samples' OD value at 490 nm was determined by the Model 680 Microplate Reader. In order to guarantee the accuracy, each sample was seeded into 3 wells to obtain a mean value. The cell viability was calculated by comparison with the OD value of untreated cells.

2.5. Scanning Electron Microscope. Samples of treated HL60 cells were fixed in 2.5% glutaraldehyde in 0.1 M phosphate buffer solution (PBS) and freeze-dried in 6°C for 6 hours. Then they were washed three times by 0.1 M phosphate buffer solution and dehydrated by ethanol solution of 30%, 50%, 70%, 90%, and 100% successively. Isoamyl acetate was used to replace the ethanol solution in cell samples and subsequently removed by CO_2 in critical point drying method. Finally, the samples were coated with platinum in automatic high vacuum coating system (QuorumQ150T ES) before observation in a ZEISS Ultra-55 scanning electron microscope.

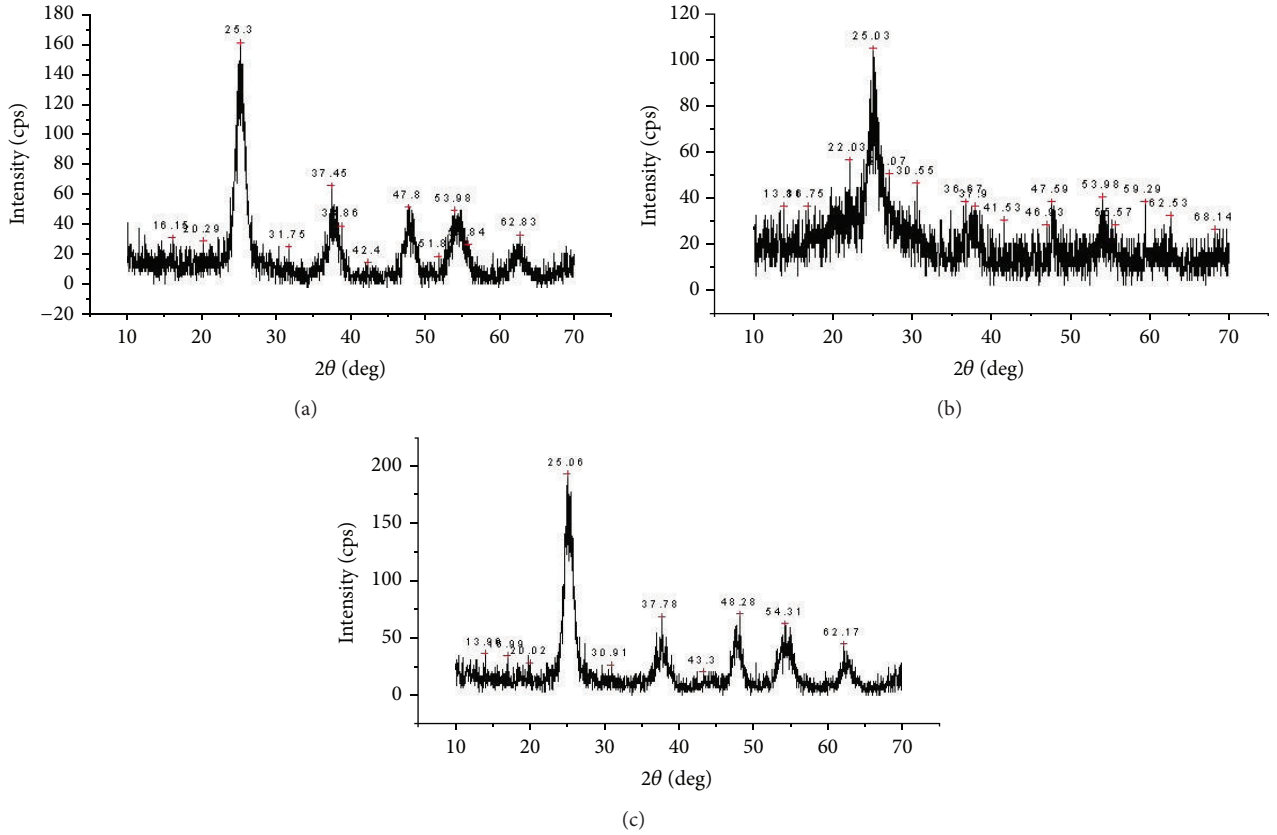

FIGURE 1: X-ray diffraction of nanoparticles: (a) pure TiO_2 nanoparticles used to synthesize 5-ALA/TiO_2; (b) Fe/TiO_2 (2%) nanoparticles; (c) Fe/TiO_2 (5%) nanoparticles.

2.6. Statistical Analysis. Data are presented as means ± SD (standard deviation) from three independent groups. Statistical software SPSS11.5 is used in statistical analysis. Any data with value P smaller than 0.05 are considered statistically significant.

3. Results and Discussion

3.1. Characterization of 5-ALA/TiO_2, Fe/TiO_2 Nanoparticles

3.1.1. X-Ray Diffraction Spectra. X-Ray diffraction is a solid method in analyzing crystalline structural properties. Thus, XRD images were taken to investigate the crystalline phases of three samples, pure TiO_2 used for the synthesis of 5-ALA/TiO_2, Fe/TiO_2 (2%), and Fe/TiO_2 (5%); they were presented in Figures 1(a), 1(b), and 1(c), respectively. Characteristic peaks in accordance with crystalline phases of (101) were found in all of the samples. Also there was no characteristic peak in (110) $2\theta = 27.4^{\circ}$, indicating that the samples are primarily in anatase phase. TiO_2 had three basic crystal phases, anatase, rutile, and brookite. It has been demonstrated that the anatase phase TiO_2 showed highest photocatalytic efficiency among the three [22, 23]. By comparison, characteristic peaks in Figure 1(b) were less crystallized; but the ones in Figures 1(a) and 1(c) were observed sharper, indicating that TiO_2 and Fe/TiO_2 (5%) were more crystallized than Fe/TiO_2 (2%).

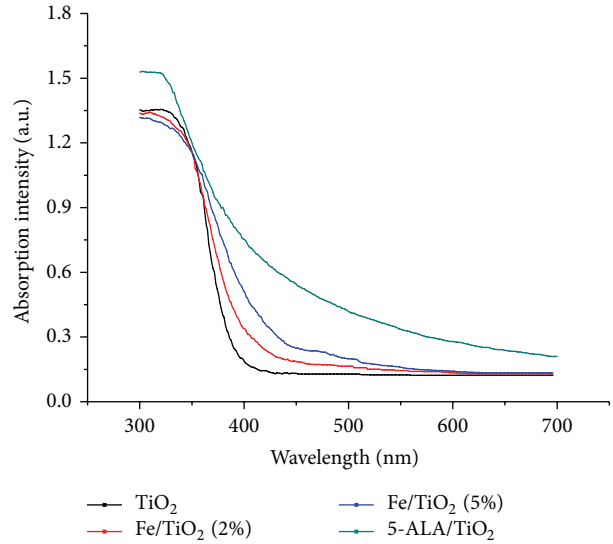

FIGURE 2: UV-Vis spectra of TiO_2, 5-ALA/TiO_2, Fe/TiO_2 (2%), and Fe/TiO_2 (5%) nanoparticles.

3.1.2. UV-Vis Spectra. UV-Vis spectra of the nanoparticles were studied to investigate their photocatalytic performance. As is shown in Figure 2, the spectrum of TiO_2 has a very sharp

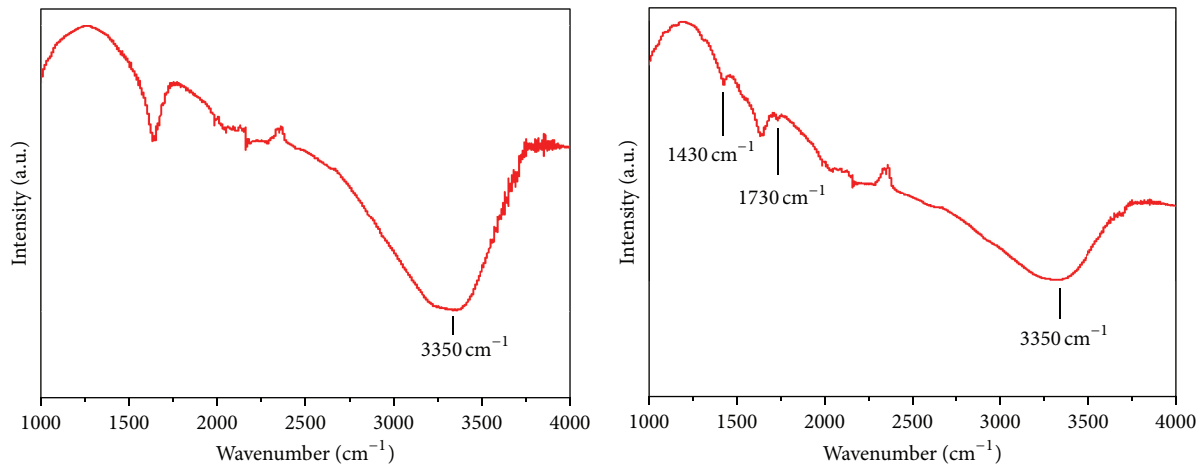

Figure 3: FTIR spectra: (a) TiO_2 nanoparticles; (b) 5-ALA/TiO_2 nanoparticles.

edge from 350 to 400 nm, presenting that TiO_2 nanoparticles absorb light primarily from ultraviolet region. UV-Vis spectra of 5-ALA/TiO_2, Fe/TiO_2 (2%), and Fe/TiO_2 (5%) were also observed; by comparison, we observed varying degrees of redshift, indicating that the light absorption of TiO_2 has been enhanced and expanded to visible light region, meaning that damage on normal cells from UV light during clinical treatments could be reduced. TiO_2 with a higher concentration of Fe ions absorbed more visible light. We also observed that the redshift of 5-ALA/TiO_2 was more obvious than the former; the absorption of visible light was largely promoted. Our result demonstrated that the modification of TiO_2 nanoparticles, especially with 5-ALA, helps enhance the visible light absorption. This phenomenon of redshift allowed photocatalytic activity of TiO_2 to be further activated by visible light irradiation.

3.1.3. FTIR Spectra of TiO_2 and 5-ALA/TiO_2. As shown in Figures 3(a) and 3(b), the FTIR spectra of TiO_2 and 5-ALA/TiO_2 were studied to characterize the modification of 5-ALA/TiO_2 nanoparticles. Characteristic peak of hydroxyl on surface of TiO_2 and 5-ALA/TiO_2 nanoparticles emerged in 3350 cm^{-1}. Further, characteristic peaks of carboxylic ester (–COOTi–) emerged in 1430 cm^{-1} and 1730 cm^{-1} in Figure 3(b). This finding illustrated that possible reaction, similar to the esters produced by chemical reactions of carboxylic acids and alcohols, might happen between 5-ALA and TiO_2. The weakening of peak 3350 cm^{-1} in Figure 3(b) demonstrated again that the potential reaction consumed part of the hydroxyl. The potential chemical equation was presented as follows:

$$\begin{aligned} &TiO_2\,(OH)\,n + y HOOC_5H_8NO\text{–}TiO_2\,(OH)\,n \\ &\quad - y\,(OOC_5H_8NO)\,y + y H_2O \end{aligned} \tag{2}$$

3.1.4. Raman Spectrum of 5-ALA/TiO_2. Raman spectrum of 5-ALA/TiO_2 was also taken to reaffirm the existence of

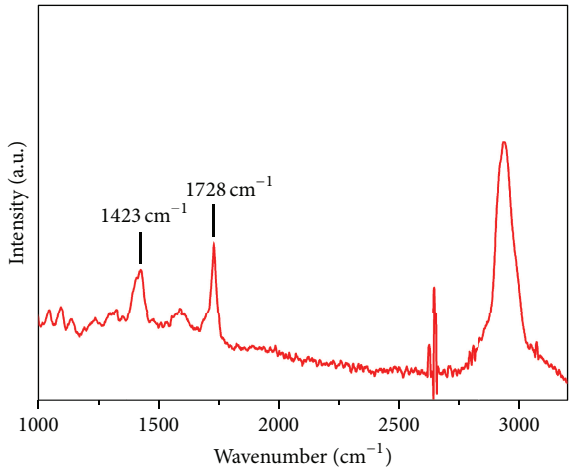

Figure 4: Raman spectrum of 5-ALA/TiO_2 nanoparticles.

carboxylic ester (–COOTi–). As shown in Figure 4, characteristic peaks of carboxylic ester could be observed more clearly in 1423 cm^{-1} and 1728 cm^{-1}, which matched the finding from the FTIR spectra in Section 3.1.3.

3.2. Cytotoxicity of Modified TiO_2 Nanoparticles on HL60. Low dark toxicity is known as one of the important features of photosensitive drugs. We ran a series of experiments to test the dark toxicity of our modified TiO_2 nanoparticles on HL60 cells. Various concentrations (0 μg/mL, 50 μg/mL, 100 μg/mL, 150 μg/mL, 200 μg/mL, 250 μg/mL, 500 μg/mL, and 1000 μg/mL) of TiO_2, Fe/TiO_2 (2%), Fe/TiO_2 (5%), and that (72.75 μg/mL, 145.50 μg/mL, 218.25 μg/mL, 291.00 μg/mL, 363.75 μg/mL, 436.50 μg/mL, 582.00 μg/mL, and 1164.00 μg/mL) of 5-ALA/TiO_2 were adopted in the test; the OD value of HL60 was measured after culturing for 48 hours, and the relative cell viability of HL60 was presented in Figure 5.

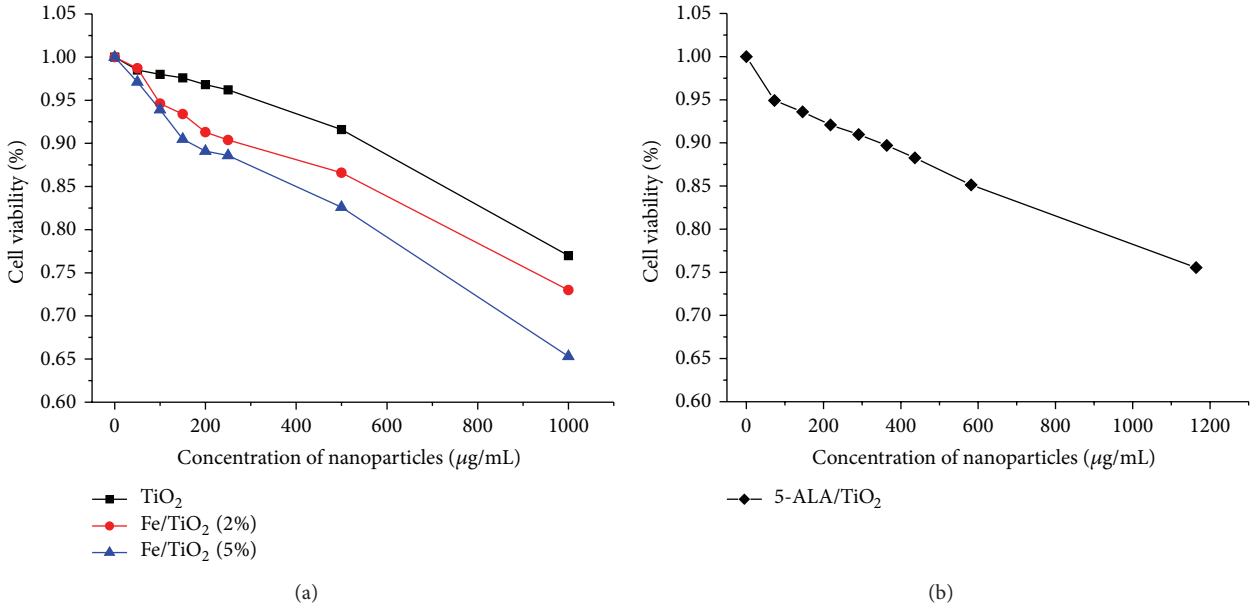

Figure 5: Effect of (a) TiO_2 and Fe/TiO_2 and (b) $5\text{-ALA}/TiO_2$ of different concentration on HL60 cell viability.

We learned that the viability of HL60 softly declines with the increase of drug concentration. That said, photosensitive drugs influenced HL60 cells viability without radiation, even though not much. In detail, TiO_2 had relatively mild inhibitory effect on HL60 until the concentration went up to 500 μg/mL, where cell viability dropped to 90%; the inhibitory effect was more obvious in groups of Fe/TiO_2 and Fe/TiO_2 (5%) appeared to have higher toxicity than Fe/TiO_2 (2%). Their cell viability dropped to 90% when the concentration of Fe/TiO_2 reached approximately 200 μg/mL. And note that the curves turned sharper at the concentration range over 200 μg/mL. From Figure 5(b), we can observe that the curve of Fe/TiO_2 (5%) dropped slightly faster than the one of Fe/TiO_2 (2%). The $5\text{-ALA}/TiO_2$ group revealed that $5\text{-ALA}/TiO_2$ nanoparticles were less toxic to HL60 cells than Fe/TiO_2, but more than pure TiO_2. The corresponding cell viability dropped to 90% when the concentration of $5\text{-ALA}/TiO_2$ reached approximately 360 μg/mL.

3.3. Photodynamic Therapy on HL60. HL60 cells in a concentration of 0.5×10^5/mL were inoculated into two 96-well plates marked as A and B. Plate A received light treatment (luminous power 5 mW/cm^2, light dose 18 J/cm^2, wavelength 403 ± 6 nm, period 1 hour) after 24-hour incubation in dark and then another 24-hour incubation in dark. Plate B, as control group, was incubated in dark for continuous 48 hours in the incubator. According to Figure 5, the final concentration we adopted was 200 μg/mL for TiO_2, Fe/TiO_2 (2%), and Fe/TiO_2 (5%) and 360 μg/mL $5\text{-ALA}/TiO_2$, for under these concentrations; the viability of HL60 cells was the same 90% in darkroom experiments. The photocatalytic effect (indicated by Pe) was expressed by cell viability, which was calculated as follows:

$$\text{Pe} = 1 - \frac{\text{OD}_{\text{treated}}}{\text{OD}_{\text{untreated}}} * 100\%, \quad (3)$$

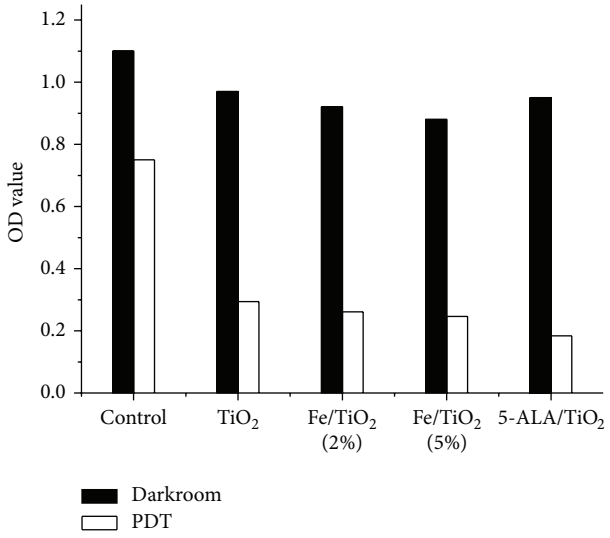

Figure 6: Effect of PDT of different nanoparticles on OD value of HL60 cells.

where the $\text{OD}_{\text{treated}}$ and $\text{OD}_{\text{untreated}}$ are the mean absorption values at 490 nm for the treated and untreated samples, respectively. Overall results were presented in Figure 6.

From Figure 6, we found that the cells viability of control group remained stable relatively. As to PDT group, cell viability dropped remarkably. To state the obvious, cell viability under light treatment of TiO_2 decreased greatly to 30.3%; furthermore, the ones of modified TiO_2 happened to reach a greater decrease. This evidence revealed that modification of Fe ion and 5-ALA enhances photocatalytic inactivation effect of TiO_2. Specifically, cell viability under $5\text{-ALA}/TiO_2$-PDT dropped to 19.4% and Fe/TiO_2 (2%) and Fe/TiO_2 (5%) to 28.4% and 28.0%, respectively. That said, Fe/TiO_2

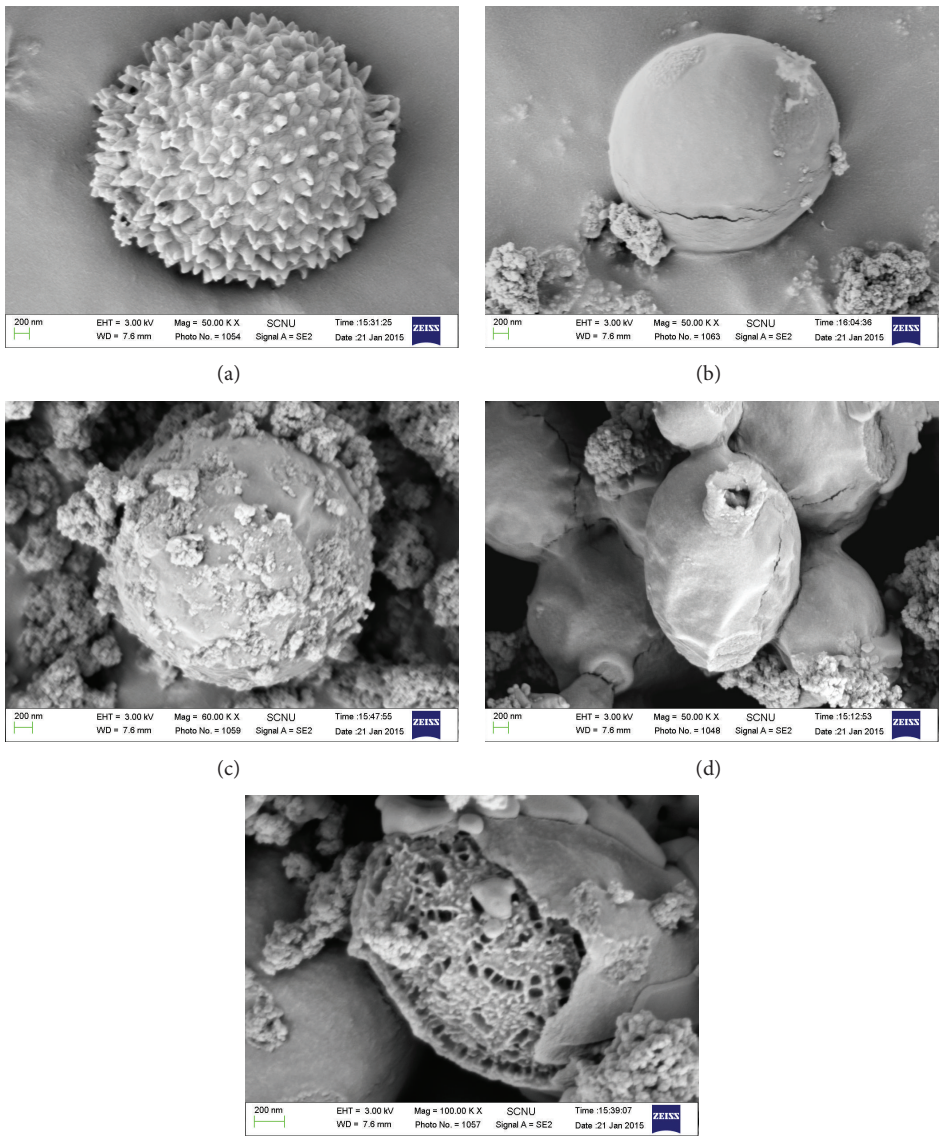

Figure 7: Ultrastructural morphology of HL60 cells: (a) normal cultured cell; (b) cell cultured with Fe/TiO_2 in darkroom; (c) cell cultured with 5-ALA/TiO_2 in darkroom; (d) PDT-treated cell cultured with Fe/TiO_2; (e) PDT-treated cell cultured with 5-ALA/TiO_2.

nanoparticles did not present obviously higher photocatalytic effect in comparison to pure TiO_2 nanoparticles. However, 5-ALA/TiO_2 present promising photocatalytic effect. For the viability of HL60 cells of each darkroom group stayed above 80%, and the one of each radiance group nearly stayed all below 30%; we found that the activation of the modified TiO_2 from PDT was the main cause of cell apoptosis.

3.4. Scanning Electron Microscope (SEM) Image of the Treated HL60 Cells. The ultrastructural morphology of HL60 cell, the ultrastructural morphology of HL60 cell cultured with Fe/TiO_2 and 5-ALA/TiO_2, and the ultrastructural morphology of PDT-treated HL60 cell cultured with 5-ALA/TiO_2 and 5-ALA/TiO_2 were shown in Figures 7(a), 7(b), 7(c), 7(d), and 7(e), respectively. In Figure 7(a), HL60 cell was observed to remain morphologically intact. In Figures 7(b) and 7(c), we observed plump HL60 cells with smooth surface, attached or covered by nanoparticles. Based on experience, cell viability was slightly influenced in this stage. In Figure 7(d), the HL60 cell surface became hollow and deform; breakage of cytomembrane was observed clearly. In Figure 7(e), the same condition emerged in HL60 cell. From it, not only the breakdown of cytomembrane but also the damage of the inner cytoplasm was obviously observed. Damaged cytoplasm was observed to have entirely extruded out from cytomembrane in certain PDT-treated cells.

4. Conclusion

In this paper, the modification of Fe and 5-ALA on TiO_2 was explored in experiments. Fe/TiO_2 (2%), Fe/TiO_2 (5%) were

synthesized by precipitation method and 5-ALA/TiO_2 was synthesized by ultrasonic method. They were all used as experimental photosensitizer in photodynamic therapy. X-ray diffraction was used to verify their anatase phase; and the UV-Vis spectrum indicated that the modification of TiO_2 leads to a redshift of absorption spectrum. Our experimental results showed that the modification of TiO_2 promotes the absorption in visible light region of TiO_2. TiO_2 and modified TiO_2 develop nearly no harm to HL60 cells when in darkroom with proper experimental doses but can still result in cell death in high concentration. Our experiment proved that modified TiO_2 nanoparticles performed a high photocatalytic effect on HL60 cells than pure TiO_2. And among all three kinds of them, 5-ALA/TiO_2 had the greatest inhibitory effect on HL60 cells. Besides, Fe/TiO_2 (5%) cause a higher inhibitory effect than Fe/TiO_2 (2%), indicating that higher proportion of Fe^+ in modified TiO_2 performs better photocatalytic effect in light treatments. Three kinds of nanoparticles, including 5-ALA/TiO_2 in 360 μg/mL, Fe/TiO_2 (2%) in 200 μg/mL, and Fe/TiO_2 (5%) in 200 μg/mL, were used in photodynamic therapy on HL60 cells for 1-hour light treatment in a luminous power of 5 mW/cm^2. Cell viability of each independent group was 19.4%, 28.4%, and 28.0% respectively, indicating that 5-ALA/TiO_2 nanoparticles had a higher inhibitory effect in the doses which caused the same dark toxicity, yet Fe/TiO_2 nanoparticles did not present obviously higher photocatalytic effect in comparison to pure TiO_2 nanoparticles.

Scanning electron microscope was used to observe the ultrastructural morphology of HL60 cells before and after PDT and the images and PDT results together showed that the synthesized nanoparticles cause obvious damage on HL60 through PDT.

Conflict of Interests

The authors declare that there is no conflict of interests regarding the publication of this paper.

Acknowledgments

This work has been financially supported by the National Natural Science Foundation of China (61072029) and Science and Technology Planning Project of Guangzhou City (2014J4100049).

References

[1] Q. X. Zhou, Z. Fang, J. Li, and M. Wang, "Applications of TiO_2 nanotube arrays in environmental and energy fields: a review," *Microporous and Mesoporous Materials*, vol. 202, pp. 22–35, 2015.

[2] S. T. Hussain and A. Siddiqa, "Iron and chromium doped titanium dioxide nanotubes for the degradation of environmental and industrial pollutants," *International Journal of Environmental Science and Technology*, vol. 8, no. 2, pp. 351–362, 2011.

[3] M. Behpour, S. M. Ghoreishi, and F. S. Razavi, "Photocatalytic aactivity of TiO_2/Ag nanoparticle on degradation of water pollutions," *Digest Journal of Nanomaterials and Biostructures*, vol. 5, no. 2, pp. 467–475, 2010.

[4] C. Wang, H. Liu, and Y. Qu, "TiO_2-based photocatalytic process for purification of polluted water: bridging fundamentals to applications," *Journal of Nanomaterials*, vol. 2013, Article ID 319637, 14 pages, 2013.

[5] T. Zubkoy, D. Stahl, T. L. Thompson, D. Panayotov, O. Diwald, and J. T. Yates Jr., "Ultraviolet light-induced hydrophilicity effect on TiO_2(110) (1 × 1). Dominant role of the photooxidation of adsorbed hydrocarbons causing wetting by water droplets," *Journal of Physical Chemistry B*, vol. 109, no. 32, pp. 15454–15462, 2005.

[6] J. Wang, Y. Guo, B. Liu et al., "Detection and analysis of reactive oxygen species (ROS) generated by nano-sized TiO_2 powder under ultrasonic irradiation and application in sonocatalytic degradation of organic dyes," *Ultrasonics Sonochemistry*, vol. 18, no. 1, pp. 177–183, 2011.

[7] N. Shimizu, C. Ogino, M. F. Dadjour, K. Ninomiya, A. Fujihira, and K. Sakiyama, "Sonocatalytic facilitation of hydroxyl radical generation in the presence of TiO_2," *Ultrasonics Sonochemistry*, vol. 15, no. 6, pp. 988–994, 2008.

[8] Y. Chihara, K. Fujimoto, H. Kondo et al., "Anti-tumor effects of liposome-encapsulated titanium dioxide in nude mice," *Pathobiology*, vol. 74, no. 6, pp. 353–358, 2007.

[9] J. Yu, L. Qi, and M. Jaroniec, "Hydrogen production by photocatalytic water splitting over Pt/TiO_2 nanosheets with exposed (001) facets," *Journal of Physical Chemistry C*, vol. 114, no. 30, pp. 13118–13125, 2010.

[10] C. M. Sayes, R. Wahi, P. A. Kurian et al., "Correlating nanoscale titania structure with toxicity: a cytotoxicity and inflammatory response study with human dermal fibroblasts and human lung epithelial cells," *Toxicological Sciences*, vol. 92, no. 1, pp. 174–185, 2006.

[11] J. Xu, Y. Sun, J. Huang et al., "Photokilling cancer cells using highly cell-specific antibody-TiO_2 bioconjugates and electroporation," *Bioelectrochemistry*, vol. 71, no. 2, pp. 217–222, 2007.

[12] T. López, M. Alvarez, R. D. González et al., "Synthesis, characterization and in vitro cytotoxicity of Pt-TiO_2 nanoparticles," *Adsorption*, vol. 17, no. 3, pp. 573–581, 2011.

[13] T. Lopez, E. Ortiz, M. Alvarez et al., "Study of the stabilization of zinc phthalocyanine in sol-gel TiO_2 for photodynamic therapy applications," *Nanomedicine: Nanotechnology, Biology, and Medicine*, vol. 6, no. 6, pp. 777–785, 2010.

[14] S. Yamaguchi, H. Kobayashi, T. Narita et al., "Novel photodynamic therapy using water-dispersed TiO_2-polyethylene glycol compound: Evaluation of antitumor effect on glioma cells and spheroids in vitro," *Photochemistry and Photobiology*, vol. 86, no. 4, pp. 964–971, 2010.

[15] Z. Li, X. Pan, T. Wang, P.-N. Wang, J.-Y. Chen, and L. Mi, "Comparison of the killing effects between nitrogen-doped and pure TiO_2 on HeLa cells with visible light irradiation," *Nanoscale Research Letters*, vol. 8, no. 1, pp. 1–7, 2013.

[16] W. Wang, Q. Shang, W. Zheng et al., "A novel near-infrared antibacterial material depending on the upconverting property of Er^{3+}-Yb^{3+}-Fe^{3+} tridoped TiO_2 nanopowder," *Journal of Physical Chemistry C*, vol. 114, no. 32, pp. 13663–13669, 2010.

[17] Z. Li, L. Mi, P.-N. Wang, and J.-Y. Chen, "Study on the visible-light-induced photokilling effect of nitrogen-doped TiO_2 nanoparticles on cancer cells," *Nanoscale Research Letters*, vol. 6, no. 1, pp. 1–7, 2011.

[18] J. Xu, Y. Sun, Y. M. Zhao, J. J. Huang, C. M. Chen, and Z. Y. Jiang, "Photocatalytic inactivation effect of gold-doped TiO_2

(Au/ TiO_2) nanocomposites on human colon carcinoma LoVo cells," *International Journal of Photoenergy*, vol. 2007, Article ID 97308, 7 pages, 2007.

[19] K. Huang, L. Chen, J. Deng, and J. Xiong, "Enhanced visible-light photocatalytic performance of nanosized anatase TiO_2 doped with CdS quantum dots for cancer-cell treatment," *Journal of Nanomaterials*, vol. 2012, Article ID 720491, 12 pages, 2012.

[20] K. Huang, L. Chen, J. Xiong, and M. Liao, "Preparation and characterization of visible-light-activated Fe-N Co-doped TiO_2 and its photocatalytic inactivation effect on leukemia tumors," *International Journal of Photoenergy*, vol. 2012, Article ID 631435, 9 pages, 2012.

[21] J. W. Xiong, H. Xiao, L. Chen, J. M. Wu, and Z. X. Zhang, "Research on different detection conditions between MTT and CCK-8," *Acta Laser Biology Sinica*, vol. 16, no. 5, pp. 526–531, 2007.

[22] K. Tanaka, M. F. V. Capule, and T. Hisanaga, "Effect of crystallinity of TiO_2 on its photocatalytic action," *Chemical Physics Letters*, vol. 187, no. 1-2, pp. 73–76, 1991.

[23] R. I. Bickley, T. Gonzalez-Carreno, J. S. Lees, L. Palmisano, and R. J. D. Tilley, "A structural investigation of titanium dioxide photocatalysts," *Journal of Solid State Chemistry*, vol. 92, no. 1, pp. 178–190, 1991.